

Geophysical Research Letters



RESEARCH LETTER

10.1029/2020GL091239

Key Points:

- The Madden-Julian Oscillation (MJO) eastward propagation speed exhibits pronounced year-to-year variability with a range of 2.5–6.5 deg/day for the period of 1900–2010
- During the winters with faster propagation speed, the MJO exhibits a larger zonal-scale than that during the slow propagation winters
- The larger MJO zonal-scale during the fast MJO propagation winters tends to be coincident with an expansion of the Indo-Pacific warm pool

Supporting Information:

- Supporting Information S1

Correspondence to:

X. Jiang and Z. Wu,
xianan@ucla.edu;
zhiweiwu@fudan.edu.cn

Citation:

Lyu, M., Jiang, X., Wu, Z., Kim, D., & Adames, Á. F. (2021). Zonal-scale of the Madden-Julian Oscillation and its propagation speed on the interannual time-scale. *Geophysical Research Letters*, 48, e2020GL091239. <https://doi.org/10.1029/2020GL091239>

Received 18 OCT 2020

Accepted 3 FEB 2021

© 2021. The Authors.

This is an open access article under the terms of the [Creative Commons Attribution-NonCommercial License](https://creativecommons.org/licenses/by-nc/4.0/), which permits use, distribution and reproduction in any medium, provided the original work is properly cited and is not used for commercial purposes.

Zonal-Scale of the Madden-Julian Oscillation and Its Propagation Speed on the Interannual Time-Scale

Mengxia Lyu^{1,2,3}, Xianan Jiang^{2,4} , Zhiwei Wu³ , Daehyun Kim⁵ , and Ángel F. Adames⁶ 

¹College of Atmosphere Sciences, Nanjing University of Information Science and Technology, Nanjing, China,

²Joint Institute for Regional Earth System Science and Engineering, University of California, Los Angeles, CA, USA,

³Department of Atmospheric and Oceanic Sciences / Institute of Atmospheric Sciences, Fudan University, Shanghai, China,

⁴Jet Propulsion Laboratory, California Institute of Technology, Pasadena, CA, USA, ⁵Department of Atmospheric Sciences, University of Washington, Seattle, WA, USA, ⁶Department of Atmospheric and Oceanic Sciences, University of Wisconsin, Madison, WI, USA

of Wisconsin, Madison, WI, USA

Abstract While no significant long-term trend in the propagation speed of the Madden-Julian Oscillation (MJO) in boreal winter is found during the past decades, pronounced year-to-year variability of the MJO phase speed is illustrated by analyzing a century-long record data set. During the winters when fast MJO propagation is observed, the MJO exhibits a much larger zonal-scale than that during the winters with slow propagation. A broader extension in MJO circulation effectively induces stronger and broader lower-tropospheric moistening (drying) to the east (west) of MJO through horizontal moisture advection, prompting a faster MJO phase speed. The larger MJO zonal-scale during the fast MJO propagation winters is coincident with anomalously increased background sea surface temperatures and precipitable water over both the western Indian Ocean and central/eastern Pacific, reminiscent of an expansion of the Indo-Pacific warm pool. A fundamental question remains open regarding the key processes that determine the zonal-scale of MJO organization.

Plain Language Summary The Madden-Julian Oscillation (MJO), the most prominent climate mode in Tropics with a prevailing period of 30–60 days, has tremendous influences on global weather extremes. Our present-day numeric climate and weather prediction models, however, remain struggling in simulating the MJO, particularly its slow eastward propagation from the Indian Ocean to the western Pacific. Meanwhile, a knowledge gap remains in understanding the essential physics in regulating this oscillation form. In this study, we examine the year-to-year variability of the MJO propagation speed by analyzing a century-long historical data set to verify the key processes for MJO propagation in the context of existing theories. While no significant climate trend in the MJO propagation speed is found during the past decades, one interesting finding is that the MJO exhibits a significantly larger zonal-scale during the winters with faster propagation speed. More effective moistening by the broadly extended anomalous easterlies to the east of the MJO is found to be critical for the faster eastward propagation. These winters with faster MJO propagation are often characterized by an expansion of the Indo-Pacific warm pool on both its eastern and western edges. A fundamental question is raised by this study regarding the intrinsic spatial-scale of the MJO organization and how it is affected by the environment in the real world.

1. Introduction

While the Madden-Julian Oscillation (MJO; Madden & Julian, 1971; 1972) exerts far-reaching influences on global weather and climate extremes (Jiang et al., 2020a; Lau & Waliser, 2012; Zhang, 2013), many salient characteristics of the observed MJO, including its slow eastward propagation of 5 deg day⁻¹ over the Indo-Pacific region, remain poorly represented in our state-of-the-art climate models (Ahn et al., 2017, 2020; Jiang et al., 2015, 2020b). Meanwhile, despite various existing MJO theories, our knowledge of fundamental MJO processes remains elusive (Jiang et al., 2020a; Zhang et al., 2020). Different mechanisms have been proposed to interpret MJO propagation, including the horizontal/vertical advection of the moist static energy or moisture (e.g., Andersen and Kuang, 2012; Adames, 2017; Adames & Wallace, 2015; Gonzalez & Jiang, 2019; Hsu & Li, 2012; Jiang, 2017; Jiang et al., 2020c; Kim et al., 2017; Maloney, 2009; Sobel et al., 2014; Yokoi & Sobel, 2015), the east-west asymmetry between the Kelvin wave (KW) and Rossby wave (RW) components coupled with MJO convection (Chen & Wang, 2018; Wang and Lee, 2017), or the

wind-induced surface heat exchange (WISHE; Fuchs & Raymond, 2017). The essential factors regulating the phase speed of MJO propagation, which can significantly influence its induced teleconnection patterns (Yadav & Straus, 2017), are not completely understood.

Based on a traditional view that considers the MJO a couplet of the equatorial KW and RW, the MJO phase speed is determined by the relative intensity of equatorial low-level anomalous KW easterlies and RW westerlies (Wang and Chen, 2017; Wang and Lee, 2017). A stronger KW component, which can be reinforced by RW responses to the suppressed MJO phase that leads enhanced MJO convection (Chen & Wang, 2018; Kim et al., 2014), promotes stronger boundary layer (BL) convergence to the east of MJO convection (Maloney & Hartmann, 1998; Wang and Li, 1994), and thus leads to faster eastward propagation of the MJO by counteracting a dragging effect by the RW component.

Meanwhile, under the moisture mode framework (Adames & Kim, 2016; Raymond & Fuchs, 2009; Sobel & Maloney, 2013), several processes have been proposed critical in regulating the MJO phase speed (Adames & Kim, 2016). These include the convective moisture adjustment time-scale (τ ; Adames, 2017; Bretherton et al., 2004; Jiang et al., 2016), static stability, zonal-scale of the MJO, and horizontal/vertical gradients of mean moisture. These factors have been examined to understand changes of the MJO propagation speed under a warming scenario in model simulations (Adames et al., 2017; Rushley et al., 2019). An increase of the MJO phase speed with warming ($\sim 2.4\% \text{ K}^{-1}$) is ascribed to the enhanced horizontal moisture advection by the steepening of the mean horizontal moisture gradient and the increase in MJO zonal-scale, which is partially offset by a longer τ and an increase in the static stability (Adames et al., 2017; Rushley et al., 2019).

Motivated by these above modeling studies on changes of MJO characteristics under a warming climate, it will be interesting to explore whether systematic changes in the MJO propagation speed is detectable in the past decades using a long-term data set. In particular, as the diversified MJO propagation behaviors have been recently reported based on statistics of individual MJO events (Wang et al., 2019), we will investigate the year-to-year variability of the MJO propagation speed and associated mechanisms in the context of the aforementioned factors. This analysis is expected to provide further insights into fundamental physics regulating propagation of the MJO.

2. Data and Methods

To investigate long-term variability in characteristics of MJO propagation, daily variables from the ERA-20C reanalysis (Poli et al., 2016) with a horizontal resolution of $1.5 \times 1.5^\circ$ from 1900 to 2010 are analyzed. While only the observed surface/sea-level pressures and surface marine winds are assimilated in ERA-20C, indices of several prominent climate variability modes in the recent decades based on ERA-20C, including the MJO, are well compared to those based on other datasets (Poli et al., 2016). Precipitation from the Tropical Rainfall Measuring Mission (TRMM; Huffman et al., 2007) during 1998–2010 and from ERA-Interim (Dee et al., 2011) during 1979–2010 are also analyzed to validate results based on ERA-20C.

Daily anomalies of each variable are derived by removing the climatological annual cycle. A time-space filtering following Wheeler and Kiladis (1999) (hereafter WK-filter) is used to extract MJO convective signals by retaining rainfall variances within 20–80 days and eastward zonal-wavenumbers 1–5. Other fields associated with the MJO are derived by regressing their 20–80-day filtered anomalies against the WK-filtered MJO rainfall index. Analyses in this study focus on the extended boreal winter (November–March).

As shown in Supplementary Figure S1, the MJO eastward propagation, derived by lag-regression of WK-filtered precipitation anomalies onto an Indian Ocean (IO) base point ($75\text{--}85^\circ\text{E}$; $5^\circ\text{S}\text{--}5^\circ\text{N}$), are largely similar between TRMM and ERA-20C during 1998–2010, although the amplitude is weaker in ERA-20C. Very similar MJO propagation characteristics between 1998–2010 and 1900–2010 are also found in ERA-20C (Figure S1b and S1c).

Similarly, as in Figure S1, the time-longitude diagram of lag-regressed WK-filtered precipitation anomalies against the IO base point for each winter can be calculated. Following Adames et al. (2016), the MJO propagation speed during each winter is estimated by the slope of precipitation extrema within ± 20 days and between $45^\circ\text{E}\text{--}150^\circ\text{E}$ using a linear-square fit (see Figure 2 for an example).

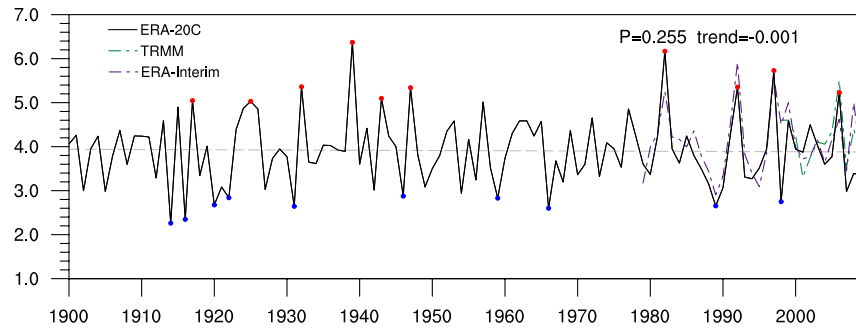


Figure 1. MJO propagation speed (deg day^{-1}) during winters from 1900 to 2010 based on ERA-20C (black), from 1979 to 2010 based on ERA-Interim (purple), and from 1998 to 2010 based on TRMM (green). Red (blue) dots denote the 10 winters with the fastest (slowest) phase speed. MJO, Madden-Julian Oscillation.

3. Results

Figure 1 illustrates that the MJO propagation speed exhibits pronounced interannual variability in winters from 1900 to 2010, with an average speed of about 4 deg day^{-1} and a range of $2.5\text{--}6.5 \text{ deg day}^{-1}$. The MJO phase speed based on ERA-20C during the recent decades are largely consistent with those based on ERA-Interim and TRMM, lending confidence to the employment of the ERA-20C data for this study. Note that no statistically significant long-term trend in the MJO propagation speed is detected during 1900–2010, which indicates that the long-term changes in the background state are not effective to make a significant projection on the MJO phase speed. This will be further discussed in Section 4.

To facilitate a comparison of MJO characteristics during winters with fast and slow MJO propagation, 10 winters with the fastest and slowest MJO phase speed are selected (Figure 1, Supplementary Table S1). Figure 2 shows composites of lag-regressed rainfall anomalies during the fast and slow MJO propagation winters, corresponding to a phase speed of 5.6 and 2.6 deg day^{-1} , respectively.

Spatial distributions of composite winter mean total precipitation (TP) and SST anomalies for each group of winters are illustrated in Figures 3a–3c. During the fast MJO winters, positive SST and precipitation anomalies are observed over both the equatorial western IO and central/eastern Pacific (CEP), while weak negative anomalies over the Indo-Pacific region. This anomalous winter mean state largely resembles conditions during the El Niño winters, indicating an expansion of the Indo-Pacific warm pool (IPWP). This is in agreement with the coincidence of several selected fast MJO propagation winters with strong El Niño years, for example, 1982/1983 and 1997/1998, and slow propagation winters with strong La Niña years, such as 1998/1999. While relatively faster (slower) MJO propagation during El Niño (La Niña) winters was recently reported by Wei and Ren (2019), most of the identified fast/slow MJO propagation winters are not associated with strong El Niño/La Niña conditions (Table S1), suggesting that the SST variability associated with El Niño/La Niña does not explain all aspects of the interannual variations of the MJO propagation speed. Similar composite results for the two groups of winters can be obtained when these several strong El Niño/La Niña events are excluded. While we focus on the bulk characteristics of MJO propagation during each winter in this study, a largely similar anomalous SST pattern as in Figure 3c is also shown to be associated with different MJO phase speed based on composites of individual MJO events (Chen & Wang, 2020; Wang et al., 2019).

Figures 3d and 3e further presents composite winter mean precipitable water (PW) and 10m-wind anomalies for the fast and slow winters. Differences in mean PW patterns between the two groups largely follow those in SSTs, with enhanced PW over the western IO and CEP, along with slightly reduced surface mean westerlies over the IO (Figure 3f). Zonal profiles of mean PW during the two groups of winters are further illustrated in Supplementary Figure S2 with significant differences evident to the west of 60°E and to the east of 170°E (Figure S2a). Differences in the mean meridional PW profiles between the two groups are not statistically significant (Figure S2b), suggesting that changes in the MJO phase speed between the fast and slow winters are not due to changes in the mean meridional moisture gradient, which was found important in affecting the simulated MJO phase speed under a warming climate (Adames et al., 2017).

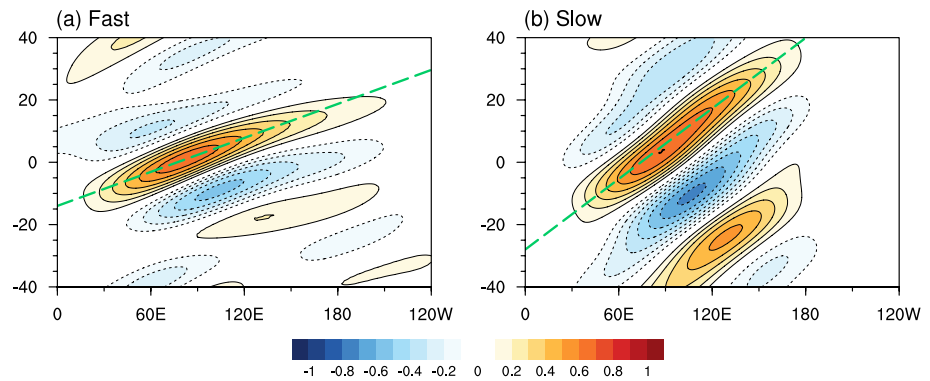


Figure 2. Longitude-time (days) evolution of rainfall anomalies (mm day^{-1}) along the equator (10°S – 10°N) for (a) the fast and (b) slow MJO propagation winters. These evolution patterns are derived by lag-regression of WK-filtered rainfall anomalies against the averaged values over the IO (75° – 85°E ; 5°S – 5°N). The MJO phase speed is indicated by the slope of rainfall anomalies (green dash lines). IO, Indian Ocean; MJO, Madden-Julian Oscillation; WK, Wheeler and Kiladis.

As previously discussed, τ and the static stability have been proposed to be important in regulating the MJO phase speed (Adames & Kim, 2016). Shown in the Supplementary Figure S3, τ , denoted by slopes in the scatterplots of WK-filtered PW and TP anomalies, are largely similar during the fast and slow winters. Additionally, the mean dry static energy over the Indo-Pacific exhibits very similar vertical profiles between these two groups (Supplementary Figure S4). Therefore, τ and the static stability may not be the essential factors responsible for the interannual variability of the MJO phase speed.

Figure 4 illustrates longitude-pressure cross-sections of MJO moisture and wind anomalies during the fast and slow winters. A typical westward-tilting structure with altitude in MJO moisture anomalies, the ascending motion coupled with MJO convection, and a descending branch to the east, are evident in both winters. A larger zonal-scale of the MJO, however, is readily discerned during the fast winters. While the MJO convection is located near 80°E in both cases, the BL moisture preconditioning to the east of MJO is detectable to the east of 120°E during the fast winters, but is confined to the west of 120°E in the slow winters. Correspondingly, the strongest descending motion to the east of MJO convection is found near 150°E during the fast winters in association with a more eastward extension of KW responses, but near 125°E during the slow winters. In

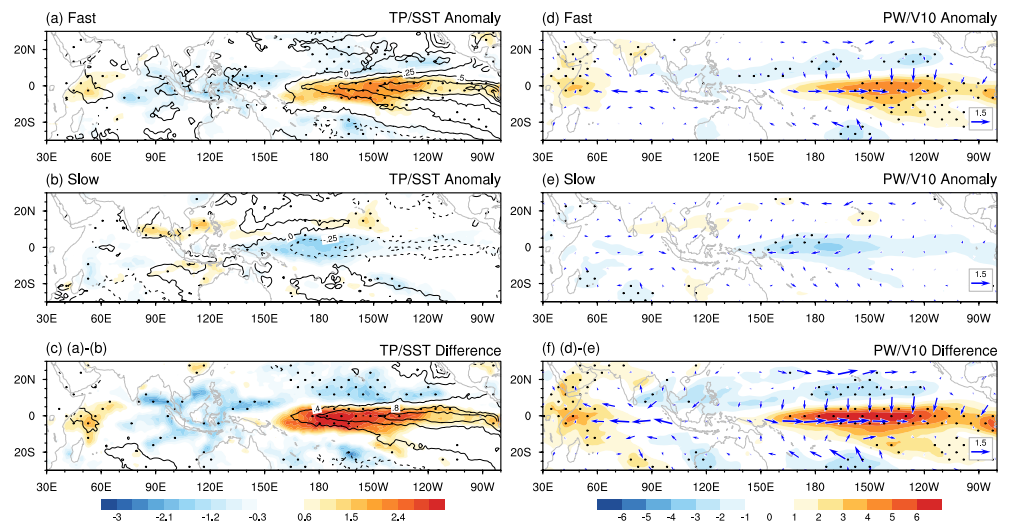


Figure 3. (left) Composite anomalous winter mean TP (shading; mm day^{-1}) and SST (contour; $^{\circ}\text{C}$), and (right) PW (mm) and 10 m winds (vectors; m s^{-1}) for the fast and slow MJO propagation winters along with their differences. Regions with stipples indicate the shaded anomalies are statistically significant at the 95% level. IO, Indian Ocean; MJO, Madden-Julian Oscillation; PW, Precipitable water; SST, sea surface temperature; TP, total precipitation.

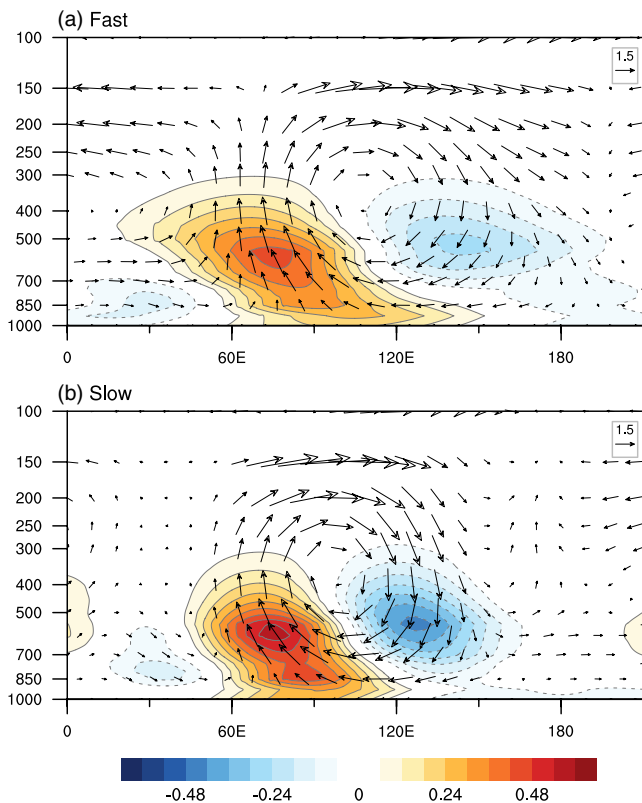


Figure 4. Longitude-pressure cross-sections of anomalous MJO horizontal wind (u) versus vertical pressure-velocity (ω , sign reversed) (vectors; see scales on the upper-right with units of m s^{-1} for u -wind, and 15 Pa s^{-1} for ω) and specific humidity (shading; g kg^{-1}) along the equator (10°S – 10°N) in the (a) fast and (b) slow MJO propagation winters. These profiles are derived by regression against WK-filtered rainfall anomalies over the IO (75° – 85°E , 5°S – 5°N). IO, Indian Ocean; MJO, Madden-Julian Oscillation; WK, Wheeler and Kiladis.

mentary Figure S5), mainly by the zonal advection (not shown), associated with the broader extension of zonal MJO winds (Figure 5d).

Note that recent composite analyses based on individual MJO events also suggested a larger zonal-scale for individual fast-propagating MJO events (Wang et al., 2019). It was proposed that the larger zonal-scale of the MJO will favor stronger KW responses and enhanced moisture preconditioning to the east of MJO convection due to BL convergence, and thus accelerate MJO eastward propagation (Chen and Wang, 2020; Wang et al., 2019). However, stronger KW easterlies to the east of MJO convection associated with the larger MJO zonal-scale are not observed in this study (Figure 5d); meanwhile, the moistening to the east of MJO extends far beyond the BL convergence region in both groups (cf., Figures 5c and 5f). While a faster MJO phase speed with increase of MJO scale is also expected by the WISHE theory (Fuchs & Raymond, 2017), considering the prevalence of winter mean surface westerlies over IO (not shown) and the presence of negative anomalous surface heat fluxes to the east of MJO convection in both groups (Supplementary Figure S6), the WISHE mechanism may not play an active role for the distinct MJO phase speed between the two groups.

4. Conclusion and Discussion

Toward improved understanding of essential physics regulating MJO propagation, the year-to-year variability of the MJO propagation speed during boreal winter is investigated by analyzing the ERA-20C reanalysis during 1900–2010. MJO phase speed exhibits pronounced interannual variability with a range of 2.5–

contrast to strong KW components associated with MJO convection, the RW response to the west of MJO convection is rather weak during the slow winters compared to that during fast winters, which is further evident in Figure 5. The weak coupling of RW and KW components associated with slow MJO propagation is in contrast to a strong RW component of the MJO during La Niña years in Wei and Ren (2019), and does not support the notion of a stronger KW versus RW component, measured by an westerly intensity index, associated with faster MJO propagation (Wang and Chen, 2017; Wang and Lee, 2017; Wei & Ren, 2019). This may indicate that the circulation-induced moisture tendencies could be important in governing the MJO propagation (Wang et al., 2018).

By the moisture mode theory, a larger zonal-scale of the MJO is associated with faster MJO eastward propagation by more effectively inducing moistening (drying) to the east (west) of the MJO through moisture advection (Adames & Kim, 2016). The dispersion relationship using a linear moisture wave suggested that the MJO phase speed is inversely proportional to the square of the zonal wavenumber (Adames & Kim, 2016). If the distance between the ascending branch over the IO and descending branch to the east as shown in Figure 4 is used to roughly estimate the MJO zonal-scale, a ratio of 1.5 in the MJO zonal-scales between the fast and slow winters (e.g., 70 vs. 45 longitude degrees) is consistent with the increased MJO phase speed from 2.6 to 5.6 deg day^{-1} from the slow to fast winters as predicted by the moisture mode theory.

Figure 5 further illustrates anomalous PW and PW tendency associated with the MJO. A much broader zonal extension and stronger amplitude in PW tendency anomalies are found during the fast MJO winters (Figures 5a–b and 5e). While the maximum moistening to the east of the MJO is found near 110°E with positive tendencies present all the way to the dateline in the fast winters, moistening is mainly confined to the west of 140°E with a maximum near 100°E during the slow winters. Similarly, drying to the west of the MJO also extends more westward during the fast winters (Figure 5e). Detailed moisture budget analysis suggests that the larger extension of PW tendencies during the fast winters is mainly due to the horizontal moisture advection in the lower-troposphere (Supple-

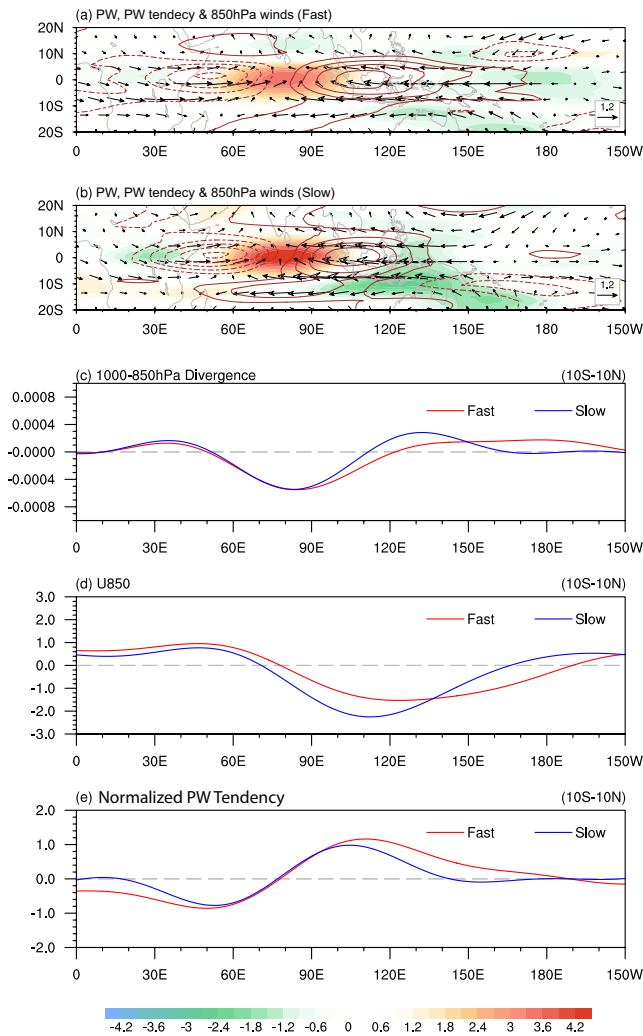


Figure 5. Spatial patterns of anomalous PW (shading; scaled by the color bar; units: mm), PW tendency (contours with an interval of 0.8 mm day^{-1}), and horizontal winds at 850 hPa (vectors; units: m s^{-1}) associated with the MJO for (a) the fast and (b) slow propagation winters. Longitudinal (10°S – 10°N average) profiles of (c) 1000–850 hPa averaged divergence (s^{-1}), (d) zonal winds at 850 hPa (m s^{-1}), and (e) normalized PW tendency (mm day^{-1} per mm) by corresponding PW anomalies over the MJO center (5°S – 5°N ; 75 – 85°E). All these anomalous fields are derived by regression against WK-filtered rainfall anomalies over IO. IO, Indian Ocean; MJO, Madden-Julian Oscillation; PW, Precipitable water; TP, total precipitation.

6.5 deg day^{-1} . Two groups of winters with the fastest and slowest MJO propagation speed are selected to discriminate key processes controlling the MJO phase speed on the interannual time-scale.

Several factors that have been previously considered critical in regulating the MJO phase speed, including the convective moisture adjustment timescale, static stability, and horizontal/vertical gradients of mean moisture, are found not responsible for the distinct MJO phase speed between these two groups of winters. Instead, the zonal-scale of the MJO is closely linked to the MJO phase speed. In the winters with faster MJO propagation, MJO exhibits a much larger zonal-scale with a broader extension of both KW easterlies and RW westerlies. The larger MJO zonal-scale can effectively induce stronger and more extended moistening (drying) to the east (west) of the MJO through horizontal moisture advection, thus promoting faster propagation of the MJO. The larger MJO zonal-scale during the fast winters are found to be coincident with warm anomalies in the mean SST pattern over both the western IO and CEP, reminiscent of an expansion of IPWP. The larger zonal-scale of the MJO during the fast MJO propagation winters and its association with an expansion of IPWP as revealed in this study are in accord with recent studies based on composite analyses of individual MJO events (e.g., Chen & Wang, 2020; Wang et al., 2019), and on influences of El Niño/La Niña on MJO propagation (Wei & Ren, 2019), although not all the winters with fast/slow MJO propagation identified in this study are associated with El Niño/La Niña conditions.

It has been recently suggested that the size of IPWP has experienced a significant increase since the early twentieth century, with an accelerated rate after 1980s (Roxy et al., 2019; Weller et al., 2016). This observed increasing trend in the size of IPWP is argued to be responsible for the reduced MJO residence time over the IO and increased MJO occurrence frequency over the western Pacific in the recent decades (Roxy et al., 2019). This trend in the MJO life cycle, however, could be exaggerated due to the blended low-frequency variability signals in the real-time multivariate MJO index used for that study (Lyu et al., 2019). While an expanding IPWP favors faster MJO propagation as suggested in this study, a statistically significant climate trend in MJO phase speed is not detectable from ERA-20C during 1900–2010 and from both ERA-20C and ERA-Interim for the period of 1979–2010. This discrepancy could be ascribed to the differences between the winter SST trend pattern associated with the expansion of IPWP and that associated with fast MJO propagation as shown in this study. While the former shows warming over the entire equatorial IO and western Pacific (Roxy et al., 2019), warm SST anomalies in the latter are mainly located over the western IO and CEP (Figure 3c).

While most of the existing MJO theories suggest the largest growth of the MJO at global wavenumber–1 (Jiang et al., 2020a), a fundamental question is raised by this study regarding the intrinsic spatial-scale of the MJO organization in the real world given the existence of the equatorial warm pool and cold tongue and how it is affected by the large-scale variability. Also, while a larger MJO zonal-scale is suggested to be conducive for faster MJO propagation, considering that the zonal-scale itself is an intrinsic characteristic of the MJO, it is possible that the larger zonal-scale of the MJO is just a manifestation of the fast propagation rather than a cause. These thus represent a gap in our understanding of the fundamental MJO physics that needs to be addressed in future studies using theoretical frameworks and model experiments.

Data Availability Statement

The ERA-20C and ERA-Interim reanalyses were downloaded from <http://apps.ecmwf.int/datasets/>. The TRMM 3B42 rainfall data was obtained from https://disc.gsfc.nasa.gov/datasets/TRMM_3B42_7/summary.

Acknowledgments:

M. Lyu and Z. Wu are supported by the National Natural Science Foundation of China (Grant No. 41790475) and National Key Research & Development Program of China (Grant No. 2016YFA0601801). X. Jiang acknowledges support by the NOAA Climate Program Office under awards NA17OAR4310261. D. Kim was supported by the NOAA CVP program (NA18OAR4310300), the DOE RGMA program (DE-SC0016223), the NASA MAP program (80NSSC17K0227), and KMA R&D Program (KMI2018-03110). ÁF. Adames was supported by NSF grant AGS-1841559.

References

- Adames, Á. F. (2017). Precipitation budget of the Madden-Julian Oscillation. *Journal of Atmospheric Sciences*, 74, 1799–1817. <https://doi.org/10.1175/JAS-D-16-0242.1>
- Adames, Á. F., & Kim, D. (2016). The MJO as a dispersive, convectively coupled moisture wave: Theory and observations. *Journal of the Atmospheric Sciences*, 73, 913–941. <https://doi.org/10.1175/JAS-D-15-0170.1>
- Adames, Á. F., Kim, D., Sobel, A. H., Del Genio, A., & Wu, J. (2017). Characterization of moist processes associated with changes in the propagation of the MJO with increasing CO₂. *Journal of Advances in Modeling Earth Systems*, 9, 2946–2967. <https://doi.org/10.1002/2017MS001040>
- Adames, Á. F., & Wallace, J. M. (2015). Three-dimensional structure and evolution of the moisture field in the MJO. *Journal of the Atmospheric Sciences*, 72, 3733–3754. <https://doi.org/10.1175/JAS-D-15-0003>
- Ahn, M.-S., Kim, D., Kang, D., Lee, J., Sperber, K. R., Gleckler, P. J., et al. (2020). MJO propagation across the maritime continent: Are CMIP6 models better than CMIP5 Models? *Geophysical Research Letters*, 47, e2020GL087250. <https://doi.org/10.1029/2020GL087250>
- Ahn, M.-S., Kim, D., Sperber, K. R., Kang, I.-S., Maloney, E., Waliser, D., et al. (2017). MJO simulation in CMIP5 climate models: MJO skill metrics and process-oriented diagnosis. *Climate Dynamics*, 49, 1–23. <https://doi.org/10.1007/s00382-017-3558-4>
- Andersen, J. A., & Kuang, Z. (2012). Moist static energy budget of MJO-like disturbances in the atmosphere of a zonally symmetric aquaplanet. *Journal of Climate*, 25(8), 2782–2804. <https://doi.org/10.1175/JCLI-D-11-00168.1>
- Bretherton, C. S., Peters, M. E., & Back, L. E. (2004). Relationships between water vapor path and precipitation over the tropical oceans. *Journal of Climate*, 17, 1517–1528. [https://doi.org/10.1175/1520-0442\(2004\)017<1517:RBWVPA>2.0.CO;2](https://doi.org/10.1175/1520-0442(2004)017<1517:RBWVPA>2.0.CO;2)
- Chen, G., & Wang, B. (2018). Effects of enhanced front walker cell on the eastward propagation of the MJO. *Journal of Climate*, 31, 7719–7738. <https://doi.org/10.1175/jcli-d-17-0383.1>
- Chen, G., & Wang, B. (2020). Circulation factors determining the propagation speed of the Madden-Julian Oscillation. *Journal of Climate*, 33, 3367–3380. <https://doi.org/10.1175/jcli-d-19-0661.1>
- Dee, D. P., Uppala, S. M., Simmons, A. J., Berrisford, P., Poli, P., Kobayashi, S., et al. (2011). The ERA-Interim reanalysis: Configuration and performance of the data assimilation system. *Quarterly Journal of the Royal Meteorological Society*, 137, 553–597. <https://doi.org/10.1002/qj.828>
- Fuchs, Ž., & Raymond, D. J. (2017). A simple model of intraseasonal oscillations. *Journal of Advances in Modeling Earth Systems*, 9, 1195–1211. <https://doi.org/10.1002/2017MS000963>
- Gonzalez, A. O., & Jiang, X. (2019). Distinct propagation characteristics of intraseasonal variability over the tropical West Pacific. *Journal of Geophysical Research: Atmosphere*, 0, 5332–5351. <https://doi.org/10.1029/2018JD029884>
- Hsu, P. C., & Li, T. (2012). Role of the boundary layer moisture asymmetry in causing the eastward propagation of the Madden-Julian Oscillation. *Journal of Climate*, 25, 4914–4931. <https://doi.org/10.1175/Jcli-D-11-00310>
- Huffman, G. J., Adler, R. F., Bolvin, D. T., Gu, G., Nelkin, E. J., Bowman, K. P., et al. (2007). The TRMM multisatellite precipitation analysis (TMPA): Quasi-global, multiyear, combined-sensor precipitation estimates at fine scales. *Journal of Hydrometeorology*, 8, 38–55. <https://doi.org/10.1175/JHM560.1>
- Jiang, X. (2017). Key processes for the eastward propagation of the Madden-Julian Oscillation based on multimodel simulations. *Journal of Geophysical Research: Atmosphere*, 122(2), 755–770. <https://doi.org/10.1002/2016JD025955>
- Jiang, X., Adames, Á. F., Kim, D., Maloney, E. D., Lin, H., Kim, H., et al. (2020a). Fifty years of research on the Madden-Julian Oscillation: Recent progress, challenges, and perspectives. *Journal of Geophysical Research: Atmosphere*, 125, e2019JD030911. <https://doi.org/10.1029/2019JD030911>
- Jiang, X., Kim, D., & Maloney, E. (2020b). Progress and status of MJO simulation in climate models and process-oriented diagnostics. In C. P. Chang, K. J. Ha, R. H. Johnson, D. Kim, G. N. Lau, & B. Wang (Eds.), *World scientific series on Asia-Pacific weather and climate*. 11. Singapore: World Scientific. Chapter 25 in *The Multiscale Global Monsoon System*. <https://doi.org/10.1142/11723>
- Jiang, X., Maloney, E., & Su, H. (2020c). Large-scale controls of propagation of the Madden-Julian Oscillation. *NPJ Climate and Atmospheric Science*, 3(1), 29. <https://doi.org/10.1038/s41612-020-00134-x>
- Jiang, X., Waliser, D. E., Xavier, P. K., Petch, J., Klingaman, N. P., Woolnough, S. J., et al. (2015). Vertical structure and physical processes of the Madden-Julian oscillation: Exploring key model physics in climate simulations. *Journal of Geophysical Research: Atmosphere*, 120, 4718–4748. <https://doi.org/10.1002/2014JD022375>
- Jiang, X., Zhao, M., Maloney, E. D., & Waliser, D. E. (2016). Convective moisture adjustment time scale as a key factor in regulating model amplitude of the Madden-Julian Oscillation. *Geophysical Research Letters*, 43, 10412–10419. <https://doi.org/10.1002/2016GL070898>
- Kim, D., Kim, H., & Lee, M.-I. (2017). Why does the MJO detour the maritime Continent during austral summer? *Geophysical Research Letters*, 44(5), 2579–2587. <https://doi.org/10.1002/2017GL072643>
- Kim, D., Kug, J.-S., & Sobel, A. H. (2014). Propagating versus nonpropagating Madden-Julian Oscillation events. *Journal of Climate*, 27, 111–125. <https://doi.org/10.1175/JCLI-D-13-00084>
- Lau, W. K.-M., & Waliser, D. E. (2012). In: *Intraseasonal variability in the atmosphere-ocean climate system*. (2nd ed.). Heidelberg, Germany: Springer, 613p. Retrieved from <https://www.springer.com/gp/book/9783642139130>
- Lyu, M., Jiang, X., & Wu, Z. (2019). A cautionary note on the long-term trend in activity of the Madden-Julian Oscillation during the past decades. *Geophysical Research Letters*, 46, 14063–14071. <https://doi.org/10.1029/2019GL086133>
- Madden, R. A., & Julian, P. R. (1971). Detection of a 40-50 Day Oscillation in Zonal Wind in Tropical Pacific. *Journal of the Atmospheric Sciences*, 28, 702–708.
- Madden, R. A., & Julian, P. R. (1972). Description of global-scale circulation cells in tropics with a 40-50-day period. *Journal of the Atmospheric Sciences*, 29, 702–708. [https://doi.org/10.1175/1520-0469\(1971\)028<0702:DOADOI>2.0.CO;2](https://doi.org/10.1175/1520-0469(1971)028<0702:DOADOI>2.0.CO;2)
- Maloney, E. D. (2009). The moist static energy budget of a composite tropical intraseasonal oscillation in a climate model. *Journal of Climate*, 22, 711–729. <https://doi.org/10.1175/2008JCLI2542.1>

- Maloney, E. D., & Hartmann, D. L. (1998). Frictional moisture convergence in a composite life cycle of the Madden-Julian Oscillation. *Journal of Climate*, *11*, 2387–2403. [https://doi.org/10.1175/1520-0442\(2002\)015<0964:AIOCLC>2.0.CO;2](https://doi.org/10.1175/1520-0442(2002)015<0964:AIOCLC>2.0.CO;2)
- Poli, P., Hersbach, H., Dee, D. P., Berrisford, P., Simmons, A. J., Vitart, F., et al. (2016). ERA-20C: An atmospheric reanalysis of the twentieth century. *Journal of Climate*, *29*, 4083–4097. <https://doi.org/10.1175/jcli-d-15-0556.1>
- Raymond, D. J., & Fuchs, Z. (2009). Moisture modes and the Madden-Julian Oscillation. *Journal of Climate*, *22*, 3031–3046. <https://doi.org/10.1175/2008jcli2739.1>
- Roxy, M. K., Dasgupta, P., McPhaden, M. J., Suematsu, T., Zhang, C., & Kim, D. (2019). Twofold expansion of the Indo-Pacific warm pool warps the MJO life cycle. *Nature*, *575*, 647–651. <https://doi.org/10.1038/s41586-019-1764-4>
- Rushley, S. S., Kim, D., & Adames, Á. F. (2019). Changes in the MJO under greenhouse gas-induced warming in CMIP5 Models. *Journal of Climate*, *32*, 803–821. <https://doi.org/10.1175/jcli-d-18-0437.1>
- Sobel, A., & Maloney, E. (2013). Moisture modes and the eastward propagation of the MJO. *Journal of the Atmospheric Sciences*, *70*, 187–192. <https://doi.org/10.1175/JAS-D-12-0189.1>
- Sobel, A., Wang, S., & Kim, D. (2014). Moist static energy budget of the MJO during DYNAMO. *Journal of the Atmospheric Sciences*, *71*(11), 4276–4291. <https://doi.org/10.1175/JAS-D-14-0052.1>
- Wang, B., & Chen, G. (2017). A general theoretical framework for understanding essential dynamics of Madden-Julian Oscillation. *Climate Dynamics*, *49*, 2309–2328. <https://doi.org/10.1007/s00382-016-3448-1>
- Wang, B., Chen, G., & Liu, F. (2019). Diversity of the Madden-Julian Oscillation. *Science Advances*, *5*, eaax0220. <https://doi.org/10.1126/sciadv.aax0220>
- Wang, B., & Lee, S.-S. (2017). MJO propagation shaped by zonal asymmetric structures: Results from 24 GCM simulations. *Journal of Climate*, *30*, 7933–7952. <https://doi.org/10.1175/jcli-d-16-0873.1>
- Wang, B., & Li, T. M. (1994). Convective Interaction with boundary-layer dynamics in the development of a tropical intraseasonal system. *Journal of the Atmospheric Sciences*, *51*, 1386–1400. [https://doi.org/10.1175/1520-0469\(1994\)051<1386:CIWBLD>2.0.CO;2](https://doi.org/10.1175/1520-0469(1994)051<1386:CIWBLD>2.0.CO;2)
- Wang, L., Li, T., & Nasuno, T. (2018). Impact of Rossby and Kelvin Wave components on MJO eastward propagation. *Journal of Climate*, *31*, 6913–6931. <https://doi.org/10.1175/jcli-d-17-0749.1>
- Wei, Y., & Ren, H.-L. (2019). Modulation of ENSO on fast and slow MJO modes during boreal winter. *Journal of Climate*, *32*, 7483–7506. <https://doi.org/10.1175/jcli-d-19-0013.1>
- Weller, E., Min, S.-K., Cai, W., Zwiers, F. W., Kim, Y.-H., & Lee, D. (2016). Human-caused Indo-Pacific warm pool expansion. *Science Advances*, *2*, e1501719. <https://doi.org/10.1126/sciadv.1501719>
- Wheeler, M., & Kiladis, G. N. (1999). Convectively coupled equatorial waves: Analysis of clouds and temperature in the wavenumber-frequency domain. *Journal of the Atmospheric Sciences*, *56*, 374–399. [https://doi.org/10.1175/1520-0469\(1999\)056<0374:CCEWAO>2.0.CO;2](https://doi.org/10.1175/1520-0469(1999)056<0374:CCEWAO>2.0.CO;2)
- Yadav, P., & Straus, D. M. (2017). Circulation response to fast and slow MJO episodes. *Monthly Weather Review*, *145*, 1577–1596. <https://doi.org/10.1175/mwr-d-16-0352.1>
- Yokoi, S., & Sobel, A. H. (2015). Intraseasonal variability and seasonal march of the moist static energy budget over the eastern maritime continent during CINDY2011/DYNAMO. *Journal of the Meteorological Society of Japan. Ser. II*, *93A*, 81–100. <https://doi.org/10.2151/jmsj.2015-041>
- Zhang, C. (2013). Madden-Julian Oscillation: Bridging weather and climate. *Bulletin of the American Meteorological Society*, *94*, 1849–1870. <https://doi.org/10.1175/bams-d-12-00026.1>
- Zhang, C., Adames, Á. F., Khouider, B., Wang, B., & Yang, D. (2020). Four theories of the Madden-Julian Oscillation. *Reviews of Geophysics*, *58*(3), e2019RG000685. <https://doi.org/10.1029/2019RG000685>